Propagation Hanle effect of quadrupole polaritons in Cu_2O

S. A. Moskalenko[1] and M. A. Liberman[2,3]
[1]*Institute of Applied Physics of the Academy of Sciences of Republic Moldova Academy str. 5, Kishinev MD 2028, Moldova*
[2]*Department of Physics, Uppsala University, Box 530, S-751 21, Uppsala, Sweden*
[3]*P. Kapitsa Institute for Physical Problems, Russian Academy of Sciences, 117334, Moscow, Russia*
(Received 14 February 2001; revised manuscript received 5 June 2001; published 8 January 2002)

A generalized theory of the Hanle effect is developed for the case of propagation quantum beats. Time-integrated quantum beats of two polariton wave packets with the same group velocities and polarizations belonging to two different Zeeman components in Voigt geometry of the quadrupole-active ortho-exciton Γ_5^+ level in Cu_2O crystal give rise to the propagation Hanle effect. It is characterized by a quasiresonant dependence of the emitted light intensity on the magnetic field strength, as well as by a supplementary periodic dependence. This dependence originates from the difference of the wave vectors of the carrier waves. It has a period inversely proportional to the sample thickness and can be observed when the propagation way is larger than the light wavelength and the propagation time is shorter than the dephasing time. The interference of two monochromatic waves with the same frequencies and amplitudes but with different polarizations in both Faraday and Voigt geometries is also considered. The dispersion laws of five polariton branches with different polarizations in both geometries are obtained. The theory developed with account of the effective propagation way explains recent experimental results on quantum interference in Cu_2O.

DOI: 10.1103/PhysRevB.65.064303 PACS number(s): 71.36.+c, 78.47.+p, 42.50.Md

I. INTRODUCTION

Many years ago Hanle[1] discovered a phenomenon which soon became known as the Hanle effect. It concerned the optical properties of Hg atomic gas placed into an external static magnetic field and excited by a polarized resonant radiation. The polarization plane of the secondary radiation emitted by the atoms was turned as compared with the initial excitation polarization and the scattered light was depolarized. The polarization properties of the secondary radiation essentially depend on the geometry of the experiment especially on the light propagation direction as regards the magnetic field direction. In the Faraday geometry these directions are parallel, whereas in the Voigt geometry they are perpendicular. Hanle explained his experimental results on the basis of the classical model of a three-dimensional electron damped oscillator subjected to the action of a magnetic field. The Hanle effect happened to be a coherent quantum interference effect revealed by time-integrated spectroscopy. It is not surprising that Bohr and Heisenberg payed attention to this phenomenon from the very beginning.[2] It plays an important role in atomic as well as in solid-state spectroscopy.[2–4] For the free electrons and holes in semiconductors the optical spin orientation was considered rather than the angular moment and its projections.[5–7] The optical orientation of exciton polarization was first revealed experimentally by Gross *et al.*[8] The comprehensive review by Pikus and Ivchenko[4] contains earlier results on the Hanle effect and information about the exciton polarization and the optical alignment of the exciton transition dipole moments and will be briefly discussed below.

The main features of the Hanle effect will be demonstrated on the basis of a simple quantum mechanical model of three degenerated dipole-active exciton levels in a cubic crystal with $2p$-type exciton wave functions. The exciton energy level is split by the external magnetic field into a Zeeman triplet with orbital quantum number $l=1$ and magnetic quantum numbers $m=0,\pm 1$. Polariton effects are neglected at the beginning. Their influence is the main issue of this paper. The exciton Zeeman triplet has eigenfunctions $|1,m\rangle$ of the form

$$|1,0\rangle = z, \quad |1,\pm 1\rangle = \frac{1}{\sqrt{2}}(x \pm iy). \tag{1}$$

The corresponding eigenfrequencies are ω_0 and $\omega_{\pm 1}=\omega_0 \pm \omega_L$. Here ω_0 is the optical frequency corresponding to the exciton creation energy and ω_L is the Larmor frequency. The quantum transition dipole moments $\mathbf{d_m}=\langle 0|e\mathbf{r}|1,m\rangle$ are determined as the matrix elements of the coordinate vector $\mathbf{r}=\mathbf{e_x}x+\mathbf{e_y}y+\mathbf{e_z}z$ between the ground state of the crystal $|0\rangle$ and the exciton states $|1,m\rangle$, where $\mathbf{e_x},\mathbf{e_y},\mathbf{e_z}$ are unit vectors and e is the electron charge. Taking into account the time dependence of the exciton wave functions, the exciton transition dipole moments $\mathbf{d}_m(t)$ are

$$\mathbf{d}_0(\mathbf{t}) = d_0\mathbf{e_z}\mathbf{e}^{-\mathbf{i}\omega_0\mathbf{t}}, \quad \mathbf{d}_{\pm 1}(\mathbf{t}) = d_0\frac{1}{\sqrt{\mathbf{2}}}\cdot(\mathbf{e}_x \pm \mathbf{i}\mathbf{e_y})\mathbf{e}^{-\mathbf{i}\omega_{\pm 1}\mathbf{t}}. \tag{2}$$

They determine the possibilities to excite the exciton states by the incident radiation and at the same time they determine the polarizations of the secondary radiation. For example, the exciton states $|1,\pm 1\rangle$, being excited, are able to emit, in the z direction, circularly polarized waves with counterdirected rotations and slightly different frequencies.

We will introduce conventionally three stages of the polarization transformation. The first one is the optical excitation of the exciton states. Propagating along the magnetic field direction the incident light with $\mathbf{e_x}$ polarization will excite both Zeeman components $|1,\pm 1\rangle$ with the same amplitude and phase. Their evolution in time between the mo-

ments of excitation and secondary light emission can be considered as a second stage. The most desirable scenario of this stage could be the coherent evolution governed by the Schrödinger equation without any phase destruction. Then, in the third stage, the subsequent emission of light waves with well-defined phases gives rise to their quantum interference. In the second stage the destroying phase processes are inevitable due, for example, to exciton-phonon or exciton-impurity scatterings. Only if these processes are comparatively seldom and the corresponding dephasing time, which is called also the coherence time τ_c, is sufficiently large and comparable with the exciton lifetime τ_{ex} can one expect the appearance of coherent light waves and their quantum interference. In semiconductors one has also to distinguish between the relaxation time of the exciton center of mass, τ_p, the polarization relaxation time τ_c, and the lifetime τ_{ex}. During the elastic scattering only the directions of the wave vectors are changed, whereas the energies of the particles remain unchanged. The corresponding scattering time τ_p is shorter in comparison with another two. The lifetime for ortho-excitons is due to ortho-para exciton conversion with phonon participation as well to radiative or nonradiative exciton recombinations. The coherence time is determined by scattering processes, leading to a change of the polarization plane. It remains unchanged during the time τ_c. The influence of the exciton and photon propagation and their wave vectors on the Hanle effect must also be taken into account. In the general case the secondary emission of radiation needs a unified microscopic quantum statistical description. Nevertheless, in some cases the dephasing time can be taken into account by introducing phenomenologically the exciton level broadening γ and the damping of the emitted light intensity $2\gamma=\tau_c^{-1}$. In the framework of this approach we will suppose that the amplitudes of the emitted light at the beginning of the third stage accumulate a damping γ, depending on the light frequency ω. For two exciton states $|1,\pm1\rangle$ excited during the first stage, we can determine the light waves emitted in the third stage. Their amplitudes are proportional to their transition dipole moments $\mathbf{d}_{\pm1}$, both lying in a plane perpendicular to the light propagation direction. The resultant electric field strength of the emitted light is

$$\mathbf{E}(\mathbf{t}) \cong d_0(\mathbf{e_x}+\mathbf{ie_y})\cdot \mathbf{e}^{-\mathbf{i}\omega_{+1}\mathbf{t}-\gamma\mathbf{t}} + d_0(\mathbf{e}_x-\mathbf{ie_y})\cdot \mathbf{e}^{-\mathbf{i}\omega_{-1}\mathbf{t}-\gamma\mathbf{t}} = 2d_0 e^{-i\omega_0 t-\gamma t}\cdot[\mathbf{e_x}\cos\omega_{\mathbf{L}}\mathbf{t}+\mathbf{e_y}\sin\omega_{\mathbf{L}}\mathbf{t}]. \quad (3)$$

The quantum interference effect of two circularly polarized waves in opposite directions in a longitudinal magnetic field gives rise to a resultant wave with optical frequency ω_0 of the carrier wave and with linear polarization. Its plane slowly rotates around the axis of the magnetic field with a small Larmor frequency (Larmor precession). This fact leads to a change of the polarization direction of the emitted light compared with the initial polarization of the excitation light. The intensities of the emitted light with $\mathbf{e_x}$ and $\mathbf{e_y}$ polarizations reveal the quantum beat behavior slowly decreasing in time:

$$|E_x(t)|^2 \cong |d_0|^2 e^{-2\gamma t}\cos^2\omega_L t, \quad |E_y|^2 \cong |d_0|^2 e^{-2\gamma t}\sin^2\omega_L t. \quad (4)$$

The time-integrated intensities J_x and J_y of the emitted light in two $\mathbf{e}_x$ and $\mathbf{e}_y$ polarizations and the polarization rate R of the emitted radiation are determined as

$$J_x = 2\gamma\int_0^\infty e^{-2\gamma t}\cos^2\omega_L t\,dt, \quad J_y = 2\gamma\int_0^\infty e^{-2\gamma t}\sin^2\omega_L t,$$

$$R=\frac{J_x-J_y}{J_x+J_Y}=\int_0^\infty e^{-x}\cos 2\omega_L\tau_c x\,dx=\frac{1}{1+(2\omega_L\tau_c)^2}. \quad (5)$$

This quasiresonant dependence of the polarization rate R on the magnetic field strength is the main characteristic of the Hanle effect, which appears due to quantum interference, quantum beats, and precession of the polarization plane in Faraday geometry. In the Voigt geometry there is no precession of the polarization plane, but the quasiresonant dependence remains in one linear polarization where the quantum beats exist. For example, in a perpendicular magnetic field oriented along the $\mathbf{e_x}$ direction the exciton wave functions are $|1,0\rangle = x$ and $|1,\pm1\rangle = (1/\sqrt{2})(y\pm iz)$. The light propagating along the z direction with $\mathbf{e_y}$ polarization will excite both states $|1,\pm1\rangle$ with the same amplitudes and phases but with different frequencies. Now their transition dipole moments are $\mathbf{d}_{\pm1}(\mathbf{t}) = (d_0/\sqrt{2})(\mathbf{e_y}\pm\mathbf{ie_z})\cdot\mathbf{e}^{-\mathbf{i}\omega_{\pm1}\mathbf{t}-\gamma\mathbf{t}}$. They can generate a light field propagating along the z direction only with $\mathbf{e_y}$ polarization and with the resultant electric field strength $\mathbf{E} \cong \mathbf{d}_0\mathbf{e_y}\mathbf{e}^{-\mathbf{i}\omega_0\mathbf{t}-\gamma\mathbf{t}}\cos\omega_{\mathbf{L}}\mathbf{t}$. One can see that the polarization of the resultant wave remains the same as for the incident light, but the intensity of the emitted light undergoes quantum beats in time, which leads to a quasiresonant dependence of the time-integrated intensity on the magnetic field strength.

The optical orientation of the exciton polaritons and the observation of their polarization are possible only in the case when they, being excited inside the crystal, succeed in reaching its boundary surface without scatterings and dephasing processes. Such a possibility depends on the value of the polariton group velocity and its orientation.[4] Just this case will be considered in the present paper, taking into account polariton quantum beats in the presence of a magnetic field. The influence of a magnetic field on the optical orientation of exciton polaritons was studied experimentally in CdSe crystals by Nawrocki *et al.*[9] and Planel *et al.*[10]

The Hanle effect based on the interference of polariton wave packets will be the main issue of the present paper and we will take into account the existence of the propagation quantum beats observed experimentally in Cu_2O crystals and discussed by Frohlich *et al.*,[11,12] Langer *et al.*,[13,14] and Stolz.[15] The quantum beats effect and the Faraday and Hanle effects as well as resonant Raman scattering are closely related, being intrinsically interconnected and originating from quantum interference effects. One of them is time-resolved and others are time-integrated or stationary phenomena. All of them deal with the coherence time and quantum interference of the excited states. These effects will be considered in the present work for the particular case of ortho-exciton states in Cu_2O. Comprehensive experimental studies of quantum beats, with participation of ortho-excitons in Cu_2O,

have been published in Refs. 11–15. The authors of these papers noticed that the quantum beats originate from the coherent superposition of states, which are simultaneously and coherently excited by a short optical pulse and are characterized by a small enough energy splitting. The energy splitting of the states determines the beating frequency of the emitted light. This splitting can be determined with a high resolution, being independent of the inhomogeneous broadening,[15] whereas the phase relaxation times of the excited states can be determined from the damping of the beats.[13] The coherence time, which is also known as the dephasing time, has been measured by intervals of time during which the excited states lose their initial phases. The coherence time τ_{coh} determines the homogeneous broadening of the excited state γ by the relation $2\gamma=\hbar/\tau_{coh}$, where τ_{coh} is defined by the elastic collisions, which exclusively affect the phases and do not lead to excited-state depopulation. The total energy relaxation time or the population lifetime is usually measured by time-resolved luminescence spectroscopy.[11–15] As was emphasized in Ref. 13 the quantum beat method allows one to distinguish between coherent Raman scattering and incoherent hot luminescence. The quantum beats may occur only in the coherent Raman part of the scattering.[11,12] The exciton coherence time drastically decreases with the increase of exciton kinetic energy. One-phonon resonant Raman scattering involving the $1S$ yellow series ($1SY$) exciton in Cu_2O was studied for both stationary and pulsed excitations.[13,16,17] The polariton character of the ortho-exciton states was neglected in Refs. 16 and 17. Despite its small oscillator strength the polariton concept is necessary to understand the time dependence of the light scattering.[14] Therefore the interference of two polariton states belonging to two split Zeeman components of the Γ_5^+ level will be considered in the present paper. But even at a rather high magnetic field of the order of 1 T the spectral splitting of the exciton quadrupole emission cannot be detected because of inhomogeneous line broadening. Only the quantum beat technique makes it possible to reveal a very small energy splitting and the interference of two propagating wave packets which belong to upper and lower polariton branches with the same group velocities, demonstrating how powerful the method is. These phenomena became known as propagation quantum beats.[11–15,18] Time-integrated propagation quantum beats will give rise to the propagation Hanle effect.

The $1SY$ exciton state in Cu_2O is formed from an electron-hole pair in the conduction band with symmetry Γ_6^+ and the valence band with symmetry Γ_7^+. The exciton state is split by the electron-hole exchange interaction into a triply degenerate Γ_5^+ ortho-exciton and nondegenerate Γ_2^+ paraexciton. The oscillator strength of the exciton-photon coupling is weak due to the quadrupole-type interaction, $f=3.7\times10^{-9}$.[12] In this case a characteristic polariton structure appears due to the remarkably narrow homogeneous width of the ortho-exciton recombination line.[11] The homogeneous linewidth determined by Kono and Nagasawa[19] is $2\gamma=8$, 8 μeV at 1,6 K. Contrary to this the dispersion curve and the propagation beat signal from Cu_2O crystal were calculated in Ref. 12 using a different value of the damping constant $2\gamma=0$, 9 μeV. The splitting of the uncoupled photon and exciton dispersion curves near their crossing point and the span of the polariton branches were found at about 120 μeV in Ref. 12. In spite of the small splitting these polariton branches have a very strong dispersion within a narrow range of wave vectors.[11,12] As a consequence, the polaritons formed at the front surface of the sample with slightly different energies around the exciton resonance propagate with group velocities which strongly depend on the wave vector $v_g(k)$.[14] In the presence of a magnetic field the Γ_5^+ states split into three components characterized by magnetic quantum numbers $m=0,\pm1$. In the case of the Faraday geometry, when the laser light is parallel to the direction of the external magnetic field H_0, only the states with $m=\pm1$ are allowed in the quadrupole transitions interacting with circularly polarized light. These two states show linear Zeeman splitting $\Delta E=|g_c+g_v|\mu_B H_0$, where μ_B is the Bohr magneton and the total g factor equals 1.66 accordingly[19] or 1.78 accordingly.[13]

In the present paper we revise a theory of the Hanle effect with account of the interference of two wave packets with the same group velocity instead of two monochromatic waves. The spatial dispersion and the existence of additional waves were not taken into account in a theory of the Hanle effect.[4] The theory developed of the propagation Hanle effect takes into account from the very beginning the existence of propagation quantum beats in Cu_2O crystal, as was observed experimentally in Refs. 11–15. The paper is organized as follows. In Sec. II the polariton dispersion laws in an external magnetic field are derived. There are three polariton branches in the Voigt geometry: when the polarization is parallel to the external magnetic field and two in the perpendicular polarization. In Sec. III the time-integrated quantum beats of two quadrupole polariton wave packets are studied. It is shown that the interference of two wave packets in the Voigt geometry leads to the propagation Hanle effect, which is, in particular, characterized by the frequency and wave vector of the carrier waves and by the width and group velocity of the wave packets. We found that the time-integrated intensity of light on the rear side of the sample depends on the strength of the magnetic field due to different channels. One of them is the Zeeman splitting of the exciton level and another is the difference of the wave vectors of the carrier waves, which determines the value of the phase angle Θ. The phase angle plays the role of the argument of the periodic functions, and due to this, a periodic dependence of the light intensity on the magnetic field strength appears. To the best of our knowledge this phenomenon has not been considered before. In Sec. IV we compare the theoretical dependences obtained with the experimental results published by Kono and Nagasawa.[19]

II. QUADRUPOLE POLARITONS IN AN EXTERNAL MAGNETIC FIELD

The exciton states, originating from $3d$ states of Cu^+ ions at the top valence bands of Cu_2O crystal, are known to form triply degenerate states of the irreducible representation Γ_5^+ of the O_h group. They will be designated below as xy, xz,

and yz. We introduce also the creation and annihilation operators of excitons, $a^{\dagger}_{xy,\mathbf{k}}$, $a^{\dagger}_{xz,\mathbf{k}}$, and $a^{\dagger}_{yz,\mathbf{k}}$, and $a_{xy,\mathbf{k}}$, $a_{xz,\mathbf{k}}$, and $a_{yz,\mathbf{k}}$, where $\mathbf{k}$ is the exciton wave vector. The dipole moments $\mathbf{d}_{xy,\mathbf{k}}$, $\mathbf{d}_{xz,\mathbf{k}}$, and $\mathbf{d}_{yz,\mathbf{k}}$, describing the quadrupole transitions from the ground state of the crystal into three ortho-exciton states, depend on the components k_i of the wave vector $\mathbf{k}$ and on the unit orthogonal vectors $\mathbf{e}_j$, where $j=x,y,z$.[20] The polarization vectors $\mathbf{e}_{\mathbf{k},j}$ of the light with the same wave vector $\mathbf{k}$ can be expressed through the unit vectors $\mathbf{e}_i$ and obey to the transversality condition $(\mathbf{e}_{\mathbf{k},j}\mathbf{k})=0$, where j denotes two light transverse polarizations.

Following Ref. 20 the dipole moments can be represented as

$$\mathbf{d}_{\mathbf{ij},\mathbf{k}}=\frac{e\sqrt{v_0}}{V}\cdot\sum_{\mathbf{p}}\varphi(\mathbf{p}-\alpha\mathbf{k})\cdot\frac{1}{\mathbf{v}_0}\int_{\mathbf{v}_0}\mathbf{ds}\cdot\mathbf{U}^{*}_{\mathbf{c},\mathbf{p}}(\mathbf{s})\cdot\mathbf{s}\cdot\mathbf{U}_{\mathbf{3d},\mathbf{ij},\mathbf{p}}(\mathbf{s})$$
$$=B\cdot(\mathbf{e_i}k_j+\mathbf{e_j}k_i), \tag{6}$$

where $i\neq j=x,y,z$. Due to the quadrupole character of the quantum transitions, the dipole moments $\mathbf{d}_{\mathbf{ij},\mathbf{k}}$ are proportional to the components k_i of the wave vector $\mathbf{k}$ multiplied by the unit vector $\mathbf{e}_j$ and vice versa. Here $U_{c,\mathbf{p}}(\mathbf{s})$ and $U_{3d,ij,\mathbf{p}}(\mathbf{s})$ are the Bloch functions of the conduction and valence bands, whereas $\varphi(\mathbf{p})$ is the exciton wave function of the relative electron-hole motion in momentum representation. V and v_0 are the volumes of the crystal and unit cell, correspondingly, α is the ratio of the electron mass m_e to the exciton translational mass m_{ex}, and the constant B is proportional to the exciton wave function of the relative motion in coordinate representation $\psi(r)$ at the point $r=0$. Only small values of translational wave vectors $\mathbf{k}$ are considered, so that $B\cong\psi(0)\sqrt{v_0}$, for $ka_{ex}\ll 1$, where a_{ex} is the exciton Bohr radius.

The oscillator strengths of the corresponding quantum transitions are related to the square of the dipole moments,

$$f_{ij,\mathbf{k}}=\frac{4\pi m_0 E_g}{3e^2\hbar^2}|B|^2(\mathbf{e}_i k_j+\mathbf{e}_j k_i)^2, \tag{7}$$

where E_g is the energy gap between the lower conduction band and the top valence band of the crystal. The oscillator strength depends on the orientations of both $\mathbf{k}$ and $\mathbf{e}_{\mathbf{k},j}$ vectors and was found to be equal to $f=3.7\times10^{-9}$ in the actual region of wave vectors. The Hamiltonian describing the ortho-excitons interacting with the photons in the presence of an external magnetic field of the strength $\mathbf{H}_0$ takes the form

$$H=\sum_{\mathbf{k}}E_{or}(k)[a^{\dagger}_{xy,\mathbf{k}}a_{xy,\mathbf{k}}+a^{\dagger}_{xz,\mathbf{k}}a_{xz,\mathbf{k}}+a^{\dagger}_{yz,\mathbf{k}}a_{yz,\mathbf{k}}]+\sum_{\mathbf{k}}\sum_{j=1}^{2}\hbar ckc^{\dagger}_{\mathbf{k},j}c_{\mathbf{k},j}+\frac{i\tilde{\gamma}\hbar e}{2\mu c}G\sum_{\mathbf{k}}[H_{0,x}(a^{\dagger}_{xz,\mathbf{k}}a_{xy,\mathbf{k}}-a^{\dagger}_{xy,\mathbf{k}}a_{xz,\mathbf{k}})$$
$$+H_{0,y}(a^{\dagger}_{xy,\mathbf{k}}a_{yz,\mathbf{k}}-a^{\dagger}_{yz,\mathbf{k}}a_{xy,\mathbf{k}})+H_{0,z}(a^{\dagger}_{yz,\mathbf{k}}a_{xz,\mathbf{k}}-a^{\dagger}_{xz,\mathbf{k}}a_{yz,\mathbf{k}})]+\sum_{\mathbf{k}}\sum_{j=1}^{2}\varphi_{\mathbf{k}}[(\mathbf{d}_{xy,\mathbf{k}}\cdot\mathbf{e}_{\mathbf{k},j})(c^{\dagger}_{\mathbf{k},j}a_{xy,\mathbf{k}}+a^{\dagger}_{xy,\mathbf{k}}c_{\mathbf{k},j})$$
$$+(\mathbf{d}_{xz,\mathbf{k}}\cdot\mathbf{e}_{\mathbf{k},j})(c^{\dagger}_{\mathbf{k},j}a_{xz,\mathbf{k}}+a^{\dagger}_{xz,\mathbf{k}}c_{\mathbf{k},j})+(\mathbf{d}_{yz,\mathbf{k}}\cdot\mathbf{e}_{\mathbf{k},j})(c^{\dagger}_{\mathbf{k},j}a_{yz,\mathbf{k}}+a^{\dagger}_{yz,\mathbf{k}}c_{\mathbf{k},j})]. \tag{8}$$

Here $E_{or}(k)$ denotes the creation energy of the ortho-exciton with wave vector $\mathbf{k}$, which is supposed to be the same for all three states xy, xz, and yz. The creation and annihilation operators of the photon with wave vector $\mathbf{k}$ and polarization $\mathbf{e}_{\mathbf{k},j}$ are $c^{\dagger}_{\mathbf{k},j}$ and $c_{\mathbf{k},j}$, respectively, where $j=1,2$. In the expression (8) only the orbital Zeeman effect is taken into account, whereas the diamagnetic effect is neglected.

The orbital Zeeman effect of the exciton depends on the difference of electron and hole masses through the coefficient $\tilde{\gamma}=(m_h-m_e)/(m_h+m_e)$,[21] on the reduced exciton mass $\mu=(m_h m_e)/(m_h+m_e)$, and on the constant G, which can be expressed through the total g factor of conduction and valence electrons, $|g_c+g_v|$. The projections of the external magnetic field $\mathbf{H}_0$ are labeled as $H_{o,i}$. The constant $\varphi_{\mathbf{k}}$ together with the dipole moments $\mathbf{d}_{ij,\mathbf{k}}$ determine the exciton-photon interaction. Its value equals approximately

$$(\varphi_{\mathbf{k}})^2\approx\frac{4\pi E_g}{v_0\epsilon_{\infty}},\quad c=\frac{c_0}{\sqrt{\epsilon_{\infty}}}, \tag{9}$$

where c and c_0 are the light velocity in the medium and in the vacuum, respectively, and ϵ_{∞} is the background dielectric constant.

The motion equations for the exciton and photon operators are

$$i\hbar\frac{d}{dt}a_{xy,\mathbf{k}}=E_{or}(k)a_{xy,\mathbf{k}}+\frac{i\hbar e\tilde{\gamma}G}{2\mu c}(H_{0,y}a_{yz,\mathbf{k}}-H_{0,x}a_{xz,\mathbf{k}})$$
$$+\varphi_{\mathbf{k}}\cdot\sum_{j=1}^{2}(\mathbf{d}_{xy,\mathbf{k}}\cdot\mathbf{e}_{\mathbf{k},j})c_{\mathbf{k},j},$$

$$i\hbar\frac{d}{dt}a_{xz,\mathbf{k}}=E_{or}(k)a_{xz,\mathbf{k}}+\frac{i\hbar e\tilde{\gamma}G}{2\mu c}(H_{0,x}a_{xy,\mathbf{k}}-H_{0,z}a_{yz,\mathbf{k}})$$
$$+\varphi_{\mathbf{k}}\cdot\sum_{j=1}^{2}(\mathbf{d}_{xz,\mathbf{k}}\cdot\mathbf{e}_{\mathbf{k},j})c_{\mathbf{k},j},$$

$$i\hbar\frac{d}{dt}a_{yz,\mathbf{k}}=E_{or}(k)a_{yz,\mathbf{k}}+\frac{i\hbar e\tilde{\gamma}G}{2\mu c}(H_{0,z}a_{xz,\mathbf{k}}-H_{0,y}a_{xy,\mathbf{k}})+\varphi_{\mathbf{k}}\cdot\sum_{j=1}^{2}(\mathbf{d}_{yz,\mathbf{k}}\cdot\mathbf{e}_{\mathbf{k},j})c_{\mathbf{k},j},$$

$$i\hbar\frac{d}{dt}c_{\mathbf{k},j}=\hbar ckc_{\mathbf{k},j}+\varphi_{\mathbf{k}}\cdot[(\mathbf{d}_{xy,\mathbf{k}}\cdot\mathbf{e}_{\mathbf{k},j})a_{xy,\mathbf{k}}+(\mathbf{d}_{xz,\mathbf{k}}\mathbf{e}_{\mathbf{k},j})a_{xz,\mathbf{k}}+(\mathbf{d}_{yz,\mathbf{k}}\mathbf{e}_{\mathbf{k},j})a_{yz,\mathbf{k}}]. \quad (10)$$

Below these equations will be considered in two geometries: namely, in the Faraday and Voigt geometries. In the Faraday geometry the light wave vector, which is equal to the exciton wave vector, is parallel to the magnetic field $\mathbf{k}\|\mathbf{H}_0\|\mathbf{e}_z$. In this case the dipole moments of the quadrupole transitions become

$$\mathbf{d}_{xy,\mathbf{k}}=0,\quad \mathbf{d}_{xz,\mathbf{k}}=B\mathbf{e}_x\cdot k_z,\quad \mathbf{d}_{yz,\mathbf{k}}=B\mathbf{e}_y\cdot k_z. \quad (11)$$

The motion equations in the Faraday geometry have to be written separately for circular polarizations $\sigma^{\pm}$ with complex polarization vectors $(\mathbf{e}_x\pm i\mathbf{e}_y)$ denoted as $(1,\pm i,0)$, correspondingly

$$i\hbar\frac{d}{dt}(a_{xz,\mathbf{k}}\pm ia_{yz,\mathbf{k}})=\left(E_{or}(k)\mp\frac{\hbar e\tilde{\gamma}GH_{0,z}}{2\mu c}\right)(a_{xz,\mathbf{k}}\pm ia_{yz,\mathbf{k}})+B\varphi_{\mathbf{k}}k_z(c_{\mathbf{k},1}\pm ic_{\mathbf{k},2}),$$

$$i\hbar\frac{d}{dt}(c_{\mathbf{k},1}\pm ic_{\mathbf{k},2})=\hbar ck(c_{\mathbf{k},1}\pm ic_{\mathbf{k},2})+B\varphi_k k_z(a_{xz,\mathbf{k}}\pm ia_{yz,\mathbf{k}}),$$

$$i\hbar\frac{d}{dt}a_{xy,\mathbf{k}}=E_{or}(k)a_{xy\mathbf{k}}. \quad (12)$$

The energy splitting of two orbital Zeeman components $E_{or,\pm1}(k)=E_{or}(k)\pm\hbar\omega_L$ can be represented in the form

$$\frac{\hbar e\tilde{\gamma}GH_{0,z}}{\mu c}=|g_c+g_v|\mu_BH_{0,z}=2\hbar\omega_L, \quad (13)$$

where μ_B is the Bohr magneton and ω_L is the Larmor frequency. The total g factor was experimentally determined for Cu_2O as 1.66 (Ref. 19) and 1.78 according to Ref. 12. Two ortho-exciton states $E_{or}\mp\hbar\omega_L$ are quadrupole active under the action of circularly polarized light with $\sigma_{\pm}$ polarizations, correspondingly. The third state of the type xy with the magnetic number $m=0$ remains unchanged by the light because the dipole moment $\mathbf{d}_{xy,\mathbf{k}}$ is zero. The oscillator strengths of the quadrupole transition in the point k_0, where $\hbar ck_0=E_{or}(k_0)$, are

$$f_{xz,\mathbf{k}_0}=f_{yz,\mathbf{k}_0}=\frac{4\pi m_0E_g}{3e^2\hbar^2}|B|^2k_0^2,\quad f_{xy,\mathbf{k}}=0. \quad (14)$$

Let us consider the polariton dispersion branches in the Faraday geometry. In circular polarization σ^+ there are two polariton branches related to the exciton level $E_{or,-1}(k)$, whereas in the circular polarization σ^- there is another pair of polariton branches related to the exciton level $E_{or,+1}(k)$. Their dispersion curves are derived here without taking into account the antiresonant terms. They can be described by the common formula but with different exciton energies and magnetic quantum numbers $m=\pm1$, corresponding to different Zeeman components quadrupole active in circular clockwise and counter clockwise polarizations:

$$[\hbar\omega-E_{or,\pm1}(k)](\hbar\omega-\hbar ck)=\varphi^2|B|^2k^2. \quad (15)$$

Two pairs of polariton branches are independent of each other and correspond to different circular polarizations. In many aspects they are similar to the polariton branches in the case of dipole-active exciton states but with one essential difference, which concerns the longitudinal-transverse splitting Δ_{LT} proportional to the oscillator strength of the corresponding exciton quantum transition. In the dipole-active case Δ_{LT} does not depend on wave number k and it does not vanish at the point $k=0$. In the quadrupole-active case $\Delta_{LT}\cong f_{ij,\mathbf{k}}\cong k^2$ and vanishes at the point $k=0$. But it is important in the actual point k_0 of the intersection of the exciton and photon branches determined by the equality $\hbar ck_0=E_{or}(k_0)$. The value of $f_{ij,\mathbf{k}_0}$ was determined as $f_{ij,\mathbf{k}_0}=3.7\times10^{-9}$.

The dispersion relation of the quadrupole polaritons, which was used in Ref. 12 [expression (1) in Ref. 12], differs only slightly from formula (15). To make our dispersion relation similar to the above mentioned, one can multiply the left-hand sides of the dispersion relations by the factors $[\omega+\omega_{or,\pm1}(k)](\omega+ck)/\omega^2$, whereas the right-hand sides of the equation must be multiplied by factor of 4. It is the most probable value of the factors introduced on the left-hand side and corresponds to the intersection point k_0, where $\omega\cong\omega_{or,\pm1}(k_0)\cong ck_0$, and the relation $E_{or,\pm1}(k)=\hbar\omega_{or,\pm1}(k)$ was used. Using the definitions (7) and (9) of the oscillator strength and of the coefficient φ_k^2, introducing the background dielectric constant ε_∞ instead of the value 1, which corresponds to the vacuum, and the plasmon frequency of the valence band electrons,

$$\omega_p^2=\frac{4\pi e^2}{\varepsilon_\infty v_0m_0}=\frac{(\omega_p^0)^2}{\varepsilon_\infty}, \quad (16)$$

we obtain the final expression for the dispersion law, dielectric constant $\epsilon(k,\omega)$, and square refractive index $n^2(k,\omega)$:

$$\epsilon(k,\omega)=n^2(k,\omega)=\frac{c_0^2k^2}{\omega^2}=\varepsilon_\infty+\frac{f_{or,\pm1}(k)(\omega_p^0)^2}{\omega_{or,\pm1}^2(k)-\omega^2}. \quad (17)$$

In the above expression $(\omega_p^0)^2$ is the square of the plasmon frequency contrary to a similar expression in Ref. 12. Supposing that the measured value of the quadrupole transition oscillator strength corresponds to the actual point k_0, one can write $f_{or,\pm1}(k_0)=3.7\times10^{-9}$. Then one can conclude that the numerator of the dispersion equation (17) is greater than that in Ref. 12 by the factor $(\omega_p^0)^2/c^2k_0^2$, which will be important for the following numerical estimations of the refrac-

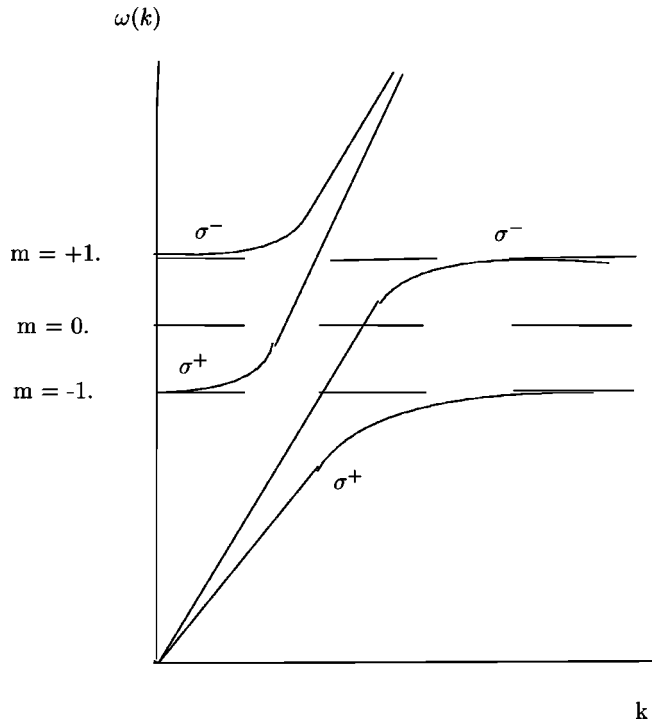

FIG. 1. The dispersion curves of two pairs of quadrupole polariton branches in the Faraday geometry and for $\sigma^{\pm}$ polarizations.

tive indexes $n(k,\omega)$ and phase angle Θ. Only in the case $\omega_p^0 = c_0 k_0$ do these two expressions coincide.

The dispersion curves of two pairs of polariton branches are presented in Fig. 1. The fifth branch is a pure exciton branch, which does not interact with the light. Each pair of polariton branches is related only to one Zeeman component and does not interact with other components. For example, the polariton branches with the circular polarization σ^+ are related to the Zeeman component with magnetic quantum number $m=-1$ and vice versa. One can observe that even in the absence of spatial dispersion, which means an infinite exciton translational mass ($m_{ex}=\infty$) at any frequency ω, there are two polariton branches with opposite circular polarizations $\sigma^{\pm}$ and with different wave vectors $k_{\pm}$. The spatial dispersion effects lead to the appearance of additional waves, as well as to the necessity to introduce additional boundary conditions. We will not consider these effects.

Let us consider the dispersion laws in the Voigt geometry. Here again the exciton and photon wave vectors are equal to each other and oriented along the z axis, $\mathbf{k}\|\mathbf{e}_z\|\langle 0,0,1\rangle$. The magnetic field $\mathbf{H}_0$ is supposed to be parallel to the x axis, $\mathbf{H}_0\|\mathbf{e}_x\|\langle 1,0,0\rangle$. This means $H_{0,x}\neq 0$ and $k_z\neq 0$ but other components are zero. As previously, the dipole moments are $\mathbf{d}_{xz,\mathbf{k}}=Bk_z\mathbf{e}_x$, $\mathbf{d}_{yz,\mathbf{k}}=Bk_z\mathbf{e}_y$, and $\mathbf{d}_{xy,\mathbf{k}}=0$. The motion equations (10) can be divided into two groups. One group contains only the photon operators with $\mathbf{e}_x$ polarization, and another one contains only the photon operators with $\mathbf{e}_y$ polarization. The first group consists of three equations

$$i\hbar\frac{d}{dt}(a_{xy,\mathbf{k}}+ia_{xz,\mathbf{k}}) = (E_{or}(k)-\hbar\omega_L)(a_{xy,\mathbf{k}}+ia_{xz,\mathbf{k}})+i\varphi_{\mathbf{k}}Bk_z c_{\mathbf{k},1},$$

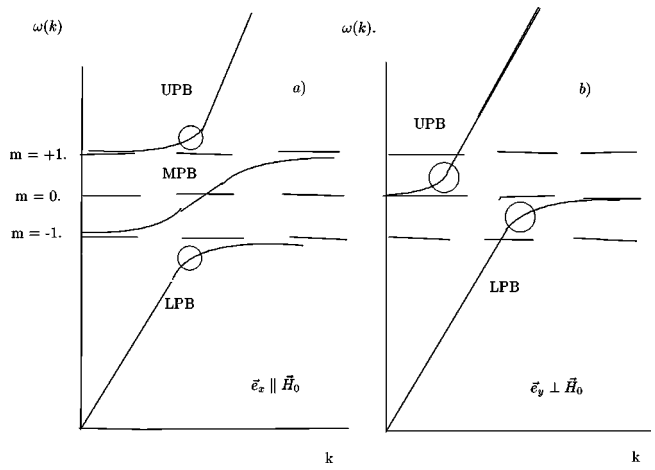

FIG. 2. The quadrupole polariton branches in the case of the Voigt geometry: (a) The case of parallel polarization: (b) The case of perpendicular polarization.

$$i\hbar\frac{d}{dt}(a_{xy,\mathbf{k}}-ia_{xz,\mathbf{k}}) = (E_{or}(k)+\hbar\omega_L)(a_{xy,\mathbf{k}}-ia_{xz,\mathbf{k}})-i\varphi_{\mathbf{k}}Bk_z c_{\mathbf{k},1},$$

$$i\hbar\frac{d}{dt}c_{\mathbf{k},1}=\hbar ckc_{\mathbf{k},1}-\frac{i\varphi_{\mathbf{k}}Bk_z}{2}(a_{xy,\mathbf{k}}+ia_{xz,\mathbf{k}}) + \frac{i\varphi_k Bk_z}{2}(a_{xy,\mathbf{k}}-ia_{xz,\mathbf{k}}). \quad (18)$$

The second group consists of two equations. It involves the photon operator with polarization $\mathbf{e}_y$ and the exciton state with magnetic quantum number $m=0$. The equations are

$$i\hbar\frac{d}{dt}a_{yz,\mathbf{k}}=E_{or}(k)a_{yz,\mathbf{k}}+\varphi_{\mathbf{k}}Bk_z c_{\mathbf{k},2},$$

$$i\hbar\frac{d}{dt}c_{\mathbf{k},2}=\hbar ckc_{\mathbf{k},2}+\varphi_{\mathbf{k}}Bk_z a_{yz,\mathbf{k}}. \quad (19)$$

In the Voigt geometry there are three split Zeeman components with magnetic quantum numbers $m=0,\pm 1$ and with corresponding energies $E_{or}(k)$ and $E_{or,\pm 1}(k)=\hbar\omega_{or,\pm 1}(k)=E_{or}(k)\pm\hbar\omega_L$. But contrary to the Faraday geometry they are constructed from other components of the initial orthoexciton states. The polariton dispersion laws for two linear polarizations are completely different. In the parallel polarization $\mathbf{e}_x\|\mathbf{H}_0\|(1,0,0)$ the dispersion law consists of three branches

$$(\omega-ck)[\omega-\omega_{or,+1}(k)][\omega-\omega_{or,-1}(k)] = \frac{\varphi_{\mathbf{k}}^2|B|^2k^2}{\hbar^2}[\omega-\omega_{or}(k)], \quad (20)$$

which is shown in Fig. 2(a). The lower polariton branch (LPB) is situated lower than the Zeeman component $E_{or,-1}(0)$, the upper polariton branch (UPB) is situated higher than the Zeeman component $E_{or,+1}(0)$, whereas the middle polariton branch (MPB) is situated between two Zee-

man components $E_{or,\pm 1}(0)$. The splittings between the LPB and MPB as well as between the MPB and UPB depend on the magnetic field and on the polariton effect. The splitting between the UPB and LPB consists of two parts. One of them equals the splitting $2\hbar\omega_L$ between two Zeeman components and another part is determined by the polariton effect and the spans of the polariton branches.

The dependence $\omega_{upb}(k)$ in the vicinity of the frequency $\omega_{or,+1}(0)$ can be obtained analytically in two limiting cases. When Zeeman splitting is more important than the polariton effect, one can approximate the expression $[\omega-\omega_{or,-1}(k)]$ by $2\omega_L$ and the difference $[\omega-\omega_{or}(k)]$ by ω_L. The dispersion law for the UPB in this approximation is

$$(\omega_{upb}-ck)[\omega_{upb}-\omega_{or,+1}(k)]=\frac{\varphi_{\mathbf{k}}^2|B|^2k^2}{2\hbar^2}. \qquad (21)$$

A similar simplification can be achieved in the range of the LPB in the vicinity of the frequency $\omega_{or,-1}(0)$:

$$(\omega_{lpb}-ck)[\omega_{lpb}-\omega_{or,-1}(k)]=\frac{\varphi_{\mathbf{k}}^2|B|^2k^2}{2\hbar^2}. \qquad (22)$$

The dispersion laws (21) and (22) look similar to Eq. (15) and can be transformed into expressions of the type (17) but with smaller by factor of 2 oscillator strengths, because the MPB situated between the frequencies $\omega_{or,\pm 1}$ becomes more developed and spread. The oscillator strengths of the quantum transitions are shared between two adjacent polariton branches. In the opposite limit of small magnetic field, when the Zeeman splitting is smaller than the polariton effect one can put approximately $(\omega-\omega_{or,\pm 1})\cong(\omega-\omega_{or})$ and may reduce Eq. (20) to Eq. (23), which will be discussed below. In the perpendicular polarization $\mathbf{e}_y\perp\mathbf{H}_0$ there are two polariton branches centered near the exciton frequency $\omega_{or}(0)$, which correspond to the $m=0$ Zeeman component. They have the dispersion law

$$(\omega-ck)[\omega-\omega_{or}(k)]=\frac{\varphi_{\mathbf{k}}^2|B|^2k^2}{\hbar^2}, \qquad (23)$$

which is shown in Fig. 2(b). One can see from Fig. 2(a) and 2(b) that there is only one wave with a given frequency for each linear polarization if one neglects spatial dispersion effects. There are two waves with the same frequency but with different reciprocal perpendicular polarizations $\mathbf{e}_x$ and $\mathbf{e}_y$. Another feature is the existence of a large spectrum of group velocities on the UPB and LPB which alter in the intervals between the light velocity in the background and infinitesimal value when the translational exciton mass is infinite. As was mentioned above only this case will be considered below. Unlike this the MPB in Fig. 2(a) has only small group velocities incomparable with the light velocity c and with the group velocities on the actual parts of the UPB and LPB. Just on these regions designated by loops is it possible to find two wave packets with the same but considerably large group velocities comparable with the light velocity c.

III. INTERFERENCE OF POLARITON WAVES AND WAVE PACKETS

In this section the main attention will be given to the time-integrated interference effect of two wave packets with the same group velocity in the Voigt geometry. We will show that this process gives rise to the propagation Hanle effect and can explain the experimental results by Kono and Nagasawa.[19]

For the beginning it should be noticed that in the case of Faraday geometry the interference of two waves with the same frequencies ω and amplitudes A, but with different circular polarizations $\sigma^{\pm}$ and wave vectors $k_{\pm}$ gives rise to one linearly polarized wave. Its polarization plane is determined by the azimuth angle $\varphi(z)$, which linearly changes its value in different points z along the propagation direction,[22] which is known as the Faraday effect:

$$\varphi(z)=\frac{k_--k_+}{2}z=\frac{[n_-(\omega)-n_+(\omega)]\omega}{2c_0}z, \quad k_{\pm}=\frac{n_{\pm}(\omega)\omega}{c_0}. \qquad (24)$$

The refractive indexes $n_{\pm}(\omega)$ can be found using the dispersion relation (17). For the parameters $d=0{,}1$ cm, $\omega/c_0=10^5$ cm^{-1}, and $\Delta n=n_-(\omega)-n_+(\omega)=10^{-4}$ we will find the azimuth $\varphi(d)=0{,}5$ rad. In the Voigt geometry the interference of two monochromatic waves with the same frequency and amplitude, but with different wave vectors $\mathbf{k}_1$ and $\mathbf{k}_2$ and polarizations $\mathbf{e}_\mathbf{x}$ and $\mathbf{e}_\mathbf{y}$, correspondingly, gives rise to a resultant wave propagating along the z direction with the same frequency but with a compound effective polarization

$$\mathbf{e}_{eff}=\frac{1}{\sqrt{2}}(\mathbf{e}_x+e^{i(k_2-k_1)z}\mathbf{e}_y). \qquad (25)$$

It changes its character and orientation, becoming linear of the type $(\mathbf{e}_x\pm\mathbf{e}_y)/\sqrt{2}$ or circular of the type $(\mathbf{e}_x\pm i\mathbf{e}_y)/\sqrt{2}$ in some points of the propagation direction, where the phase $(k_2-k_1)z$ equals $2\pi m$, $\pi(2m+1)$ and $(2m+1)\pi/2$, correspondingly. Similar polarization leads to a Sisyfus-type cooling effect in the case discussed in Ref. 23, promoting the realization of Bose-Einstein condensation of the alkali atom gases.[24] Figures 2(a) and 2(b) demonstrate that the most pronounced effect can be expected when the frequency ω lies in the spectral interval between the Zeeman components $m=\pm 1$, where the difference (k_2-k_1) is maximal.

We will consider now the interference of two wave packets with the same polarization and with the same group velocity, which is important for the propagation Hanle effect. The normalized one-dimensional wave packet can be constructed following Ref. 25 with the dispersion law of the wave frequency $\omega(k)$ taken into account. Notice that in same cases the dispersion of the damping constant $\gamma(k)$ also can be important and it will be taken into account from the very beginning to find the conditions when this dependence can or can not be neglected [see, e.g., Ref. 26 about the polariton damping constants $\gamma(k)$].

Let us introduce the wave packet as follows:

$$E(z,t)=\frac{1}{2\Delta k}\int_{k_0-\Delta k}^{k_0+\Delta k}E(k)e^{-i\omega(k)t+ikz-\gamma(k)t}dk$$

$$\cong E(k_0)e^{-i\omega(k_0)t+ik_0z-\gamma(k_0)t}\frac{[e^{i(x-i\xi)}-e^{-i(x-i\xi)}]}{2i(x-i\xi)}, \tag{26}$$

where we used the power series expansion of the dispersion law $\omega(k)$ and of the damping function $\gamma(k)$ in the vicinity of the point k_0 and the notation x and ξ,

$$\omega(k)=\omega(k_0)+v_g(k_0)(k-k_0), \quad \gamma(k)=\gamma(k_0)+s(k_0)(k-k_0),$$

$$v_g(k_0)=\left.\frac{d\omega(k)}{dk}\right|_{k=k_0}, \quad s(k_0)=\left.\frac{d\gamma(k)}{dk}\right|_{k=k_0},$$

$$x=\Delta k[v_g(k_0)t-z], \quad \xi=\Delta k s(k_0)t. \tag{27}$$

One can neglect the dispersion of $\gamma(k)$ if it changes slowly along the wave packet width $2\Delta k$ as well as if it changes more slowly than the frequency $\omega(k)$ in the same region of wave vectors. This means that the following conditions must be satisfied:

$$|s(k_0)|<\frac{\gamma(k_0)}{2\Delta k}, \quad v_g(k_0)\gg|s(k_0)|. \tag{28}$$

Taking into account that the decay time of the wave packet and its coherence (or dephasing) time is $[\tau_c=1/2\gamma(k_0)]$, one can conclude that during the most important period of time when the interference effect and quantum beats take place, the variable $\xi(\tau_c)=\Delta k s(k_0)\tau_c=\Delta k s(k_0)/2\gamma(k_0)$ is less than unity. This permits to use the power series expansion of the type $e^{\pm\xi}=1\pm\xi$ and to transform Eq. (26) as

$$E(z,t)=E(k_0)e^{-i\omega(k_0)t+ik_0z-\gamma(k_0)t}\times\left\{\frac{x\sin x}{x^2+\xi^2}+\frac{ix\xi}{x^2+\xi^2}\left(\frac{\sin x}{x}-\cos x\right)\right\}. \tag{29}$$

For a sufficiently high values of the group velocity, $v_g(k_0)>2\gamma(k_0)d$, one can put $x\cong v_g(k_0)t\Delta k$ and arrive at the inequality $x>\xi$ in correspondence to the conditions (28). In these limits and taking into account the accepted restrictions, the wave packet (29) will be used in the simplified form

$$E(z,t)=E(k_0)e^{-i\omega(k_0)t+ik_0z-\gamma(k_0)t}\frac{\sin x}{x}. \tag{30}$$

According to Eq. (30) the one-dimensional wave packet is represented as a product of two parts, one of them being the carrier wave with the frequency $\omega(k_0)$, damping $\gamma(k_0)$, and wave number k_0. The other part $(\sin x)/x$ plays the role of the envelope function. The envelope function depends on the group velocity $v_g(k_0)$ and on the wave packet width Δk.

To verify the fulfillment of the conditions (28) we will start with the simplified Hamiltonian (8), taking into account only one quadrupole-active exciton state of the type

$$H_{ex-ph}=\sum_{\mathbf{k}}[\hbar\omega_{or}(k)a_{\mathbf{k}}^{\dagger}a_{\mathbf{k}}+\hbar ckc_{\mathbf{k}}^{\dagger}c_{\mathbf{k}}+\hbar\psi_k(a_{\mathbf{k}}^{\dagger}c_{\mathbf{k}}+c_{\mathbf{k}}^{\dagger}a_{\mathbf{k}})], \tag{31}$$

where the exciton-photon interaction constant $\hbar\psi_k=\varphi_k(\mathbf{d_k e_k})$ is determined by Eqs. (9) and (11). At small density of impurities and at low density of excitations the only source of the exciton and polariton state damping is the phonons. The exciton-lattice interaction has the form[27–29]

$$H_{ex\text{-}l}=\frac{i}{\sqrt{N_a}}\sum_{\mathbf{q},\mathbf{k}}\Theta(q)a_{\mathbf{k}}^{\dagger}a_{\mathbf{k+q}}(b_{\mathbf{q}}^{\dagger}-b_{-\mathbf{q}}), \tag{32}$$

where the interaction constant $\Theta(q)$ is given by the expressions (32)–(34).[27] Tait and Weiher[26] used a simplified expression for $\Theta(q)$, which in the case of acoustical phonons has the form $(2\hbar q/9Duv_0)^{1/2}C$, where D is the crystal density, u is the sound velocity, v_0 is the unit cell volume, and N_a is the number of unit cells in the crystal of volume V $\times(V=N_a v_0)$. C is the difference between the deformation potentials for electron C_e and for hole $C_h(C=C_e-C_h)$.

The polariton states can be introduced into the Hamiltonian (31), using the polariton operators $\xi_{1,\mathbf{k}}$ and $\xi_{2,\mathbf{k}}$, introducing the unitary transformation coefficients u_k and v_k and the polariton dispersion laws $\omega_1(k)$ and $\omega_2(k)$ as follows:

$$a_{\mathbf{k}}=u_k\xi_{1,\mathbf{k}}+v_k\xi_{2,\mathbf{k}}, \quad \xi_{1,\mathbf{k}}=u_k a_{\mathbf{k}}-v_k c_{\mathbf{k}},$$

$$c_{\mathbf{k}}=u_k\xi_{2,\mathbf{k}}-v_k\xi_{1,\mathbf{k}}, \quad \xi_{2,\mathbf{k}}=u_k c_{\mathbf{k}}+v_k a_{\mathbf{k}},$$

$$u_k^2=\frac{1}{2}\left(1-\frac{\Delta_k}{\Omega_k}\right), \quad v_k^2=\frac{1}{2}\left(1+\frac{\Delta_k}{\Omega_k}\right), \quad u_k^2+v_k^2=1,$$

$$\Delta_k=\omega_{or}(k)-ck, \quad \Omega_k=\sqrt{\Delta_k^2+4\psi_k^2},$$

$$\omega_1(k)=\frac{\omega_{or}(k)+ck}{2}-\frac{1}{2}\Omega_k,$$

$$\omega_2(k)=\frac{\omega_{or}(k)+ck}{2}+\frac{1}{2}\Omega_k. \tag{33}$$

Here we marked the LPB and UPB by the numbers 1 and 2, respectively. One can observe that the coefficients u_k^2 are small in the region $k<k_0$ and approach unity in the region $k\geqslant k_0$, where k_0 is the intersection point of noninteracting exciton and photon branches and corresponds to $\Delta_{k_0}=0$. The coefficients v_k^2 have an opposite behavior.

The polariton-phonon interaction is described by the following Hamiltonian:

$$H_{p-l}=\frac{i}{\sqrt{N_a}}\sum_{\mathbf{k},\mathbf{q}}\Theta(q)[u_{\mathbf{k}}u_{\mathbf{k+q}}\xi_{1,\mathbf{k}}^{\dagger}\xi_{1,\mathbf{k}+q}+u_{\mathbf{k}}v_{\mathbf{k+q}}\xi_{1,\mathbf{k}}^{\dagger}\xi_{2,\mathbf{k+q}}+v_{\mathbf{k}}u_{\mathbf{k+q}}\xi_{2,\mathbf{k}}^{\dagger}\xi_{1,\mathbf{k}+\mathbf{q}}+v_{\mathbf{k}}v_{\mathbf{k+q}}\xi_{2,\mathbf{k}}^{\dagger}\xi_{2,\mathbf{k+q}}](b_{\mathbf{q}}^{\dagger}-b_{-\mathbf{q}}).$$

Each damping coefficient consists of two parts $\gamma_i(k) = \gamma_{i,1}(k) + \gamma_{i,2}(k)$. One of them corresponds to intrabranch scattering, whereas another component corresponds to interband polariton-phonon scattering.

The damping coefficients $\gamma_i(k)$ can be calculated using the Green's function method, which determines the self-energy part $\Sigma(k,\omega)$ and its imaginary part $\gamma(k,\omega)$. In the case of exciton-phonon interactions it was made in Refs. 27–29. Another way is to calculate the probabilities $\Gamma_i(k)$ of the scattering of the polaritons of the corresponding branches. This method was used by Tait and Weiher[26] for both polariton branches in the crystals of the type CdS with considerable polariton effect. They took into account the intraband and interband scatterings on the acoustical phonons for both polariton branches. The relations between the functions calculated by two methods are

$$\Gamma_i(k) = 2\gamma_i(k,\omega)\big|_{\omega=\omega_i(k)} = 2\gamma_i(k),$$

$$\Gamma_i(k) = \sum_{j=1}^{2} \Gamma_{i,j}(k), \quad \gamma_i(k) = \sum_{j=1}^{2} \gamma_{i,j}(k), \quad i = 1,2.$$

In the case of the LPB Tait and Weiher[26] found that at $T=0$ the only contribution to $\Gamma_i(k)$ results from the term

$$\Gamma_{11}(k, T=0) = \frac{8C^2k^2m_{ex}}{27\pi Du\hbar^2}, \quad k \geqslant k_0.$$

The damping $\Gamma_{11}(k, T=0)$ is even smaller in the range $k < k_0$.

Using this expression the damping $\gamma_1(k_0)$ and its derivative $s_1(k_0)$ can be calculated. For the parameters $D = 5$ g/cm^3, $u = 10^5$ cm/s; $C = 10$ eV; and $k_0 = 10^5$ cm^{-1} one finds $\Gamma_{11}(k_0) \cong 1{,}6 \times 10^9$ s^{-1}, $\hbar\Gamma_{11}(k_0) \cong 1$ μeV, which is close to the values estimated for quadrupole polaritons in Cu_2O. For the case of the UPB, the damping coefficient $\Gamma_{21}(k)$ is more important but it was not calculated in a way allowing the numerical estimate.[26] Now one can estimate the derivative $s_1(k_0) = \Gamma_{11}(k_0)/k_0 = 1{,}6 \times 10^4$ cm/s, which is much smaller than the light velocity c and $v_g(k_0) \approx 10^9$ cm/s and satisfies one of two conditions (28). The second condition (28) is satisfied for wave packet widths $\Delta k < \gamma(k_0)/s(k_0) = 5 \times 10^4$ cm^{-1}. The widths of the wave packet of interest does not exceed 10^2 cm^{-1}. The above discussed simplification for the variable x in the crystals of thickness $d = 0{,}5$ cm can be made only in the case of wave packets with group velocity $v_g(k_0) \geqslant 10^9$ cm/s. The above estimations allow us to conclude that the approximation we are using is justified for the particular case of quadrupole polaritons in Cu_2O crystals.

Tait and Weiher[26] noticed that in the expression for the probability, $\Gamma_2(k) = \Gamma_{22}(k) + \Gamma_{21}(k)$, the term $\Gamma_{22}(k)$ is very small because for the case of intraband scattering the final states belong to the photonlike region of the UPB where the group velocity is large but the density of states is small. It was shown in Ref. 30 that the density of states in the given point of the polariton dispersion law is inversely proportional to its group velocity. Thus, the main contribution to $\Gamma_2(k)$ belongs to the probability $\Gamma_{21}(k)$.[26] Though the numerical estimate of the probability $\Gamma_{21}(k)$ has not been done, the experiment by Ref. 31 indicates a very small dampings on the UPB. In Ref. 31 the needlelike luminescence line in the frame of the UPB was observed in the ZnTe crystal. This very sharp luminescence line, observed at the bottom of the UPB near the frequency $\omega_\parallel$, testifies to the existence of very small dampings on the UPB.

Below the interference of two one-dimensional wave packets with different carrier waves and envelope functions will be taken in the form of the wave packet, Eq. (30),

$$E(z,t) = E_1(k_1)\frac{\sin x_1}{x_1} e^{-i\omega_1(k_1)t + ik_1z + i\varphi_1 - \gamma_1 t} + E_2(k_2)\frac{\sin x_2}{x_2}\exp^{-i\omega_2(k_2)t + ik_2z + i\varphi_2 - \gamma_2 t}, \quad (34)$$

where $\omega_i(k_i)$, k_i, $\gamma_i = \gamma_i(k_i)$, Δk_i, and $x_i = [v_{g,i}(k_i)t - z]\Delta k_i$, and $i = 1,2$.

For coherent laser radiation, in the presence of a coherent macroscopic polariton wave, the polariton damping constants γ_i were studied in Refs. 32, 27, and 33. The steady-state solutions of the kinetic equations describing the mean occupation numbers of the scattered polaritons as well as of the Fokker-Planck equation describing the coherently excited polaritons of one selected mode of the crystallite were obtained in Refs. 32 and 27, taking into account the polariton-polariton interaction. The coefficients of these equations depend on the dispersive and absorptive self-energy parts, which determine the energy spectrum of the interacting polaritons and their damping coefficients. They are determined by the participation of four polaritons in the scattering process, two in the initial state and two in the final state. When both two initial polaritons belong to the selected mode and have the same wave vector $\mathbf{k}_0$, the scattered polaritons have the wave vectors $\mathbf{k}_0 \pm \mathbf{k}$. Such a conversion becomes possible only for well-defined initial and final states due the constraints imposed by energy and momentum conservation laws.[27] If between four polaritons only one belongs to the selected mode, the conservation laws can be satisfied easier. The case of the polariton-phonon interaction was investigated by Keldysh and Tikhodeev,[33] taking into account the Stokes and anti-Stokes scattering processes with the participation of the acoustical phonons. The stimulated Mandelstam-Brillouin scattering process was revealed. Numerical estimates of the relevant coefficients for the case of excitons in CdS crystals and polariton-polariton interaction were discussed in Refs. 32 and 27. For the case of quadrupole polaritons in Cu_2O crystals, one can notice that there are two estimates of the summary damping constant $2\gamma = \gamma_1 + \gamma_2$ equal to 8.8 μeV (Ref. 19) and 0.9 μeV (Ref. 12). It is important that the interference term playing the main role in the Hanle effect depend only on the summary damping constant, as will be seen below, and not depend on the damping constants γ_1 and γ_2 separately. In our calculations we will use the experimental results of both Refs. 12 and 19.

The intensity of the electric field is

$$I(z,t)=I_1(k_1)\frac{\sin^2 x_1}{x_1^2}e^{-2\gamma_1 t}+I_2(k_2)\frac{\sin^2 x_2}{x_2^2}e^{-2\gamma_2 t}$$
$$+2\sqrt{I_1(k_1)I_2(k_2)}\,\frac{\sin x_1}{x_1}\,\frac{\sin x_2}{x_2}\cos(\Omega t-\Theta)e^{-2\gamma t}, \tag{35}$$

where

$$\Omega=\omega_2(k_2)-\omega_1(k_1),\quad \Theta=(k_2-k_1)z+(\varphi_2-\varphi_1),$$
$$2\gamma=\gamma_1+\gamma_2. \tag{36}$$

As was shown in Refs. 11–15, the propagation quantum beats take place only between two wave packets with the same group velocity. They propagate from the illuminated side to the rear side of the sample, achieving the latter simultaneously and taking part in the quantum interference process. By this reason we will consider below only the case of wave packets with the same group velocity,

$$v_{g,1}(k_1)=v_{g,2}(k_2)=v_g. \tag{37}$$

For the sake of simplicity we will consider only the wave packets with the same width in the space of wave numbers and put $\Delta k_1=\Delta k_2=\Delta k$. The time integral of the expression (35) determines the time-averaged intensity of the light emitted by the illuminated side of the crystal and propagated to the rear side of the sample at the distance $z=d$, where the analyzer is located. The resultant interference effects depend essentially on the value of the crystal thickness d. One can note that the interference takes place between many pairs of wave packets and each of them has a proper group velocity. If they start at the same time on the illuminated side, they will arrive at the rear side with different time delays. This fact was observed experimentally in Cu_2O crystal, where the propagation quantum beats of quadrupole polaritons were revealed for the first time.[11–15] The group velocity along the polariton branches changes in a wide interval of values. For example, on the LPB in the range of wave numbers k smaller than the wave number k_0 of the intersection of noninteracting exciton and photon branches the group velocities are large and comparable with the light velocity, whereas in the range $k>k_0$ they are small or practically zero, if the spatial dispersion effects can be neglected. Contrary to this, on the UPB the group velocities for $k>k_0$ are of the order of the light velocity, whereas in the range $k<k_0$ they are small. Even in the absence of the spatial dispersion the UPB dispersion curve in this region is quadratic. By this reason two wave packets—one lying on the UPB and another on the LPB, being chosen with a large and equal group velocity—will have a significant frequency splitting. They will arrive first at the rear side and will result in quantum beats with relatively small periods of oscillation. They determine the initial stage of the time-resolved evolution of the propagation quantum beats. Two polariton wave packets with smaller group velocities will have a smaller frequency splitting. They will arrive at the rear side of the sample, if starting at the same time on the illuminated side, with larger time delay, and will result in quantum beats with greater periods of oscillation. This difference of the oscillation periods at the initial and final stages of the time-resolved quantum beat evolution stimulated the authors of Refs. 11–15 to introduce the notation of propagation quantum beats.

We consider pairs with large group velocities, when their propagation time through the sample is shorter than the coherence time. In this case the scattering processes can be neglected. At the same time new features of the propagation quantum beat and time-integrated evolutions appear. The behavior of the wave packets with small group velocities and propagation times larger than the coherence time mathematically does not differ from the case of two monochromatic waves. But their interference will be destroyed by the scatterings along the propagation way. These wave packets do not contribute to the propagation Hanle effect. There exists a cutoff from below for the group velocity of the wave packets. The cutoff value depends on the sample thickness. The time integral of the expression (35) cannot be calculated exactly due to the envelope functions. Taking into account that the coherence time τ_{coh} and the corresponding damping constant 2γ determine the time interval, which gives the main contribution to the time integral, one can consider two limiting cases. For the case of small group velocity $v_g<2\gamma d$, when the propagation time is larger than the coherence time $\tau_{pr}>\tau_{coh}$, the argument in Eq. (35) can be simplified:

$$x=(v_g t-d)\Delta k\approx(v_g\tau_{coh}-d)\Delta k\cong -d\,\Delta k. \tag{38}$$

In the opposite case of large group velocity $v_g>2\gamma d$ and for $\tau_{pr}<\tau_{coh}$ an estimate for x is

$$x=(v_g t-d)\Delta k\approx v_g\Delta k\, t. \tag{39}$$

In the first case $\tau_{pr}>\tau_{coh}$, the time-integrated expression (35) is similar to the case of two monochramatic waves, except for an additional constant factor. It follows from the fact that the wave packets with small group velocities are smooth and nearly monochromatic. In this case the final expression for the time integral is

$$2\gamma\int_0^\infty I(d,t)dt$$
$$=\frac{\sin^2(d\Delta k)}{(d\Delta k)^2}\left[I_1\frac{\gamma}{\gamma_1}+I_2\frac{\gamma}{\gamma_2}\right.$$
$$\left.+2\sqrt{I_1 I_2}\left(\cos\Theta\,\frac{(2\gamma)^2}{\Omega^2+(2\gamma)^2}+\sin\Theta\,\frac{2\gamma\Omega}{\Omega^2+(2\gamma)^2}\right)\right], \tag{40}$$

where

$$\Omega=\omega_2(k_2)-\omega_1(k_1),\quad \Theta=(k_2-k_1)d+\varphi,\quad \varphi=\varphi_2-\varphi_1. \tag{41}$$

The phase angle Θ in Eqs. (41) depends on the difference between the wave numbers k_i, which determine the propagation of the considered waves. To select their values it is necessary to have a supplementary condition, which we will discuss below. But even now, one can expect that the phase

angle Θ will depend on the strength of the magnetic field H_0. For the large group velocity $v_g > 2\gamma d$, the time-dependent expression $I(d,t)$ can be obtained using the dimensionless variable $\tau = v_g \Delta k\, t$ and the approximation $x \approx \tau$:

$$I(p,p_i,\Theta,\tau) = \frac{\sin^2\tau}{\tau^2}[I_1 e^{-p_1\tau} + I_2 e^{-p_2\tau} + 2\sqrt{I_1 I_2}(\cos\Theta\cos b\tau + \sin\Theta\sin b\tau)e^{-p\tau}], \tag{42}$$

where we used the designations

$$p = \frac{2\gamma}{v_g\Delta k}, \quad p_i = \frac{2\gamma_i}{v_g\Delta k}, \quad b = \frac{\Omega}{v_g\Delta k}. \tag{43}$$

To find the time-integrated expression (42) we will use Ref. 35 as well as the method proposed by Khadzhi,[34] to obtain the following formula:

$$J(p,p_i,\Theta,b) = p\{I_1 J_c(p_1,0) + I_2 J_c(p_2,0) + 2\sqrt{I_1 I_2}[\cos\Theta\, J_c(p,b) + \sin\Theta\, J_s(p,b)]\}. \tag{44}$$

Integrals in Eq. (44) are

$$\begin{aligned} J_c(p,b) &= \int_0^\infty \frac{\sin^2 x}{x^2}\cos bx\exp(-px)dx \\ &= \frac{b+2}{4}\arctan\frac{b+2}{p} + \frac{b-2}{4}\arctan\frac{b-2}{p} \\ &\quad - \frac{b}{2}\arctan\frac{b}{p} + \frac{p}{8}\ln\frac{p^2+b^2}{(b+2)^2+p^2} \\ &\quad + \frac{p}{8}\ln\frac{p^2+b^2}{(b-2)^2+p^2}, \end{aligned} \tag{45}$$

$$\begin{aligned} J_s(p,b) &= \int_0^\infty \frac{\sin^2 x}{x^2}\sin bx\exp(-px)dx \\ &= \frac{p}{4}\arctan\frac{b+2}{p} + \frac{p}{4}\arctan\frac{b-2}{p} - \frac{p}{2}\arctan\frac{b}{p} \\ &\quad + \frac{b+2}{8}\ln[(b+2)^2+p^2] + \frac{b-2}{8}\ln[(b-2)^2+p^2] \\ &\quad - \frac{b}{4}\ln(b^2+p^2). \end{aligned} \tag{46}$$

These expressions but without a square of the envelope function are[35]

$$2\gamma\int_0^\infty \exp(-2\gamma t)\cos\Omega t\, dt = \frac{(2\gamma)^2}{\Omega^2+(2\gamma)^2},$$

$$2\gamma\int_0^\infty \exp(-2\gamma t)\sin\Omega t\, dt = \frac{2\gamma\Omega}{\Omega^2+(2\gamma)^2}. \tag{47}$$

Equation (44) can be applied in both cases of light polarization $\mathbf{e}_x$ and $\mathbf{e}_y$. However, for $\mathbf{e}_x$ polarization the energy splitting between the polariton branches in Fig. 2 is determined by the Zeeman and polariton effects and increases with the increase of the magnetic field H_0. In case of $\mathbf{e}_y$ polarization Ω and b do not depend on H_0 and are determined only by the polariton splitting. As was mentioned above, the expression (40) as the function of Ω has an explicit quasiresonant form. Similar structure but with one essential difference has Eq. (44). Namely in Eq. (40) the value Ω is comparable to the damping 2γ, whereas in Eq. (44) the parameter b is determined by Eq. (43). It shows that the splitting Ω is divided by the wave packet spectral width $v_g\Delta k$. This feature becomes clear if we use the power series expansions of the integrals $J_i(p,b)$:

$$\begin{aligned} J_c(p,0) &= \arctan\frac{2}{p} + \frac{p}{4}\ln\frac{p^2}{(p^2+4)}, \\ J_c(p,b\to 0) &= J_c(p,0) - \frac{b^2}{p(p^2+4)}, \\ J_s(p,b\to 0) &= \frac{b}{4}\ln\frac{(p^2+4)}{p^2}, \\ \lim_{b\to\infty} J_i(p,b) &= 0, \quad i = c,s. \end{aligned} \tag{48}$$

Then the light intensity $J(p,\Theta,b)$ depends on the dimensionless variable $b\to 0$ as

$$\begin{aligned} &J(p,p_i\Theta,b\to 0) \\ &= p[I_1 J_c(p_1,0) + I_2 J_c(p_2,0) + 2\sqrt{I_1 I_2}\cos\Theta J_c(p,0)] \\ &\quad + 2\sqrt{I_1 I_2}\left[-\cos\Theta\frac{b^2}{p^2+4} + \sin\Theta\,\frac{b}{4}\,p\ln\frac{p^2+4}{p^2}\right]. \end{aligned} \tag{49}$$

In the opposite limit $b\to\infty$, we find

$$\lim_{b\to\infty} J(p,p_i,\Theta,b) = p[I_1 J_c(p_1,0) + I_2 J_c(p_2,0)]. \tag{50}$$

To obtain an increasing dependence of $J(p,p_i,\Theta,b)$ on b, with a very slight asymmetry, as was observed experimentally by Kono and Nagasawa,[19] it is necessary to suppose that the following inequalities $\cos\Theta < 0$ and $\sin\Theta \cong 0$ hold. The validity of these inequalities will be discussed in Sec. IV. geometry.

IV. FREQUENCY SPLITTING AND PHASE ANGLE IN VOIGT GEOMETRY

The frequency splitting Ω and phase angle Θ in the Voigt geometry and $\mathbf{e}_x$ polarization can be determined on the basis of the third-order equation (20). The dispersion laws in the ranges of the UPB and LPB can be determined approximately on the basis of the more simple Eqs. (21) and (22) with one-half of the oscillator strength in the case of a strong magnetic field and on the basis of an equation of the type (23) with full oscillator strength in the case of a weak magnetic field. Both these limiting cases can be united in the form of Eqs. (21) and (22) with effective oscillator strengths. They will be determined using the perturbation theory when the polariton effect exceeds the Zeeman splitting. Equation (20) in the range of the UPB can be rewritten in the form

$$(\omega_u - ck)(\omega_u - \omega_{or,+1}) = \frac{F_0(k)}{4} \frac{(\omega_u - \omega_{or})}{(\omega_u - \omega_{or,-1})}, \quad (51)$$

where the constant $F_0(k)$ is related to the oscillator strength of the exciton quadrupole transition $f(k)$ as follows:

$$\frac{f(k)\omega_p^2}{4} = \frac{\varphi_k^2 |B|^2 k^2}{\hbar^2}, \quad F_0(k) = f(k)\omega_p^2. \quad (52)$$

This definition of $f(k)$ differs by a factor of $\pi/3$ from the early introduced expressions (7) and (14). Here the light velocity and the plasma frequency are taken in the medium, whereas in Eq. (17) their vacuum values are used. The zero-order approximation in the case of a weak magnetic field permits us to write the equation for the UPB in the form (21). The most actual values of the UPB lie in the vicinity of the point $k_{u,0}$, which obeys the equality $ck_{u,0} = \omega_{or,+1}$. At this point the UPB frequency equals $\omega_u(k_{u,0}) = \omega_{or,+1} + \frac{1}{2}\sqrt{F_0(k_{u,0})}$. The value $\sqrt{F_0(k_{u,0})}$ determines the role of the polariton effect in the vicinity of the point $k_{u,0}$, where the propagating wave packets are selected. Substituting $\omega_u(k_{u,0})$ into the right-hand side of Eq. (52), we obtain the dispersion equation in the first-order approximation. The right-hand side of Eq. (52) becomes

$$\frac{F(k)}{4} = \frac{F_0(k)}{4} \frac{\sqrt{F_0(k_{u,0})} + 2\omega_L}{\sqrt{F_0(k_{u,0})} + 4\omega_L} = \frac{F_0(k)}{4} \eta(H_0, k_{u,0}),$$

$$\eta(H_0) = \eta(H_0, k_0) = \frac{\sqrt{F_0(k_0)} + 2\omega_L}{\sqrt{F_0(k_0)} + 4\omega_L}. \quad (53)$$

A similar result can be obtained for the LPB in the vicinity of the point $k_{l,0}$, where $ck_{l,0} = \omega_{or,-1}$ and $\omega_l(k_{l,0}) = \omega_{or,-1} - \frac{1}{2}\sqrt{F_0(k_{l,0})}$. The two expressions $\eta(H_0, k_{u,0})$ and $\eta(H_0, k_{l,0})$ are substituted by a single expression $\eta(H_0)$ with the same wave vector $k_{u,0} \simeq k_{l,0} \simeq k_0$, where $ck_0 = \omega_{or}$. The difference of three points is small in the range of magnetic fields, where the inequality $2\omega_L \leqslant \sqrt{F_0(k_0)}$ holds. The frequencies and wave numbers are designed as ω_u and k_u on the UPB and ω_l and k_l on the LPB, correspondingly. In the first-order approximation they obey

$$(\omega_u - ck_u)(\omega_u - \omega_{or,+1}) = \frac{f(k)\omega_p^2}{4} \eta(H_0),$$

$$(\omega_l - ck_l)(\omega_l - \omega_{or,-1}) = \frac{f(k)\omega_p^2}{4} \eta(H_0). \quad (54)$$

Using Eqs. (54) one can find the approximate dispersion laws on the UPB and LPB in $\mathbf{e}_x$ polarization:

$$\omega_u(k_u) = \frac{ck_u + \omega_{or,+1}}{2} + \frac{1}{2}\sqrt{(ck_u - \omega_{or,+1})^2 + F},$$

$$\omega_l(k_l) = \frac{ck_l + \omega_{or,-1}}{2} - \frac{1}{2}\sqrt{(ck_l - \omega_{or,-1})^2 + F}. \quad (55)$$

Below, the dependence $f(k)$ on k will be neglected because the derivative $df(k)/dk$ is small in the range of small k. We are interested in the values of k_u and k_l not so far situated from the point k_0 corresponding to the intersection of the exciton and photon branches $ck_0 = \omega_{or}$. Then the group velocities on two branches are

$$v_{g,u}(k_u) = \frac{c}{2} + \frac{c}{2} \frac{ck_u - \omega_{or,+1}}{\sqrt{(ck_u - \omega_{or,+1})^2 + F}},$$

$$v_{g,l}(k_l) = \frac{c}{2} - \frac{c}{2} \frac{ck_l - \omega_{or,-1}}{\sqrt{(ck_l - \omega_{or,-1})^2 + F}}. \quad (56)$$

Now we can determine the parameters of two wave packets with the same group velocities. The starting condition is the equality

$$v_{g,u}(k_u) = v_{g,l}(k_l) = v_g = \frac{c}{2}(1 + x), \quad (57)$$

where $0 \leqslant |x| < 1$. The wave numbers and frequencies are determined by

$$ck_u - \omega_{or,+1} = \frac{x}{\sqrt{1 - x^2}}\sqrt{F},$$

$$ck_l - \omega_{or,-1} = -\frac{x}{\sqrt{1 - x^2}}\sqrt{F} \quad (58)$$

and

$$\omega_u(k_u) = \omega_{or,+1} + \frac{1}{2}\sqrt{\frac{1+x}{1-x}}\sqrt{F},$$

$$\omega_l(k_l) = \omega_{or,-1} - \frac{1}{2}\sqrt{\frac{1+x}{1-x}}\sqrt{F}. \quad (59)$$

The frequency splitting $\Omega(x)$ and phase angle $\Theta(x)$ depend on the group velocity parameter x:

$$\Omega(x) = \omega_u(k_u) - \omega_l(k_l) = 2\omega_L + \sqrt{\frac{1+x}{1-x}}\sqrt{F}, \quad (60)$$

$$\Theta(x)=(k_u-k_l)d+\varphi=\frac{2\omega_L d}{c}+\frac{2xd}{c\sqrt{1-x^2}}\sqrt{F}+\varphi, \quad (61)$$

where

$$\sqrt{F}=\omega_p\sqrt{f(k_0)\,\eta(H_0)}, \quad f(k_0)=3.7\times10^{-9},$$

$$2\hbar\omega_L=|g_c+g_v|\mu_B H_0, \quad 0\leqslant|x|<1, \quad \varphi=-\pi. \quad (62)$$

In case of the Voigt geometry and $\mathbf{e}_y$ polarization formulas similar to Eqs. (61) and (62) may be used with $\omega_L=0$ and $\eta(H_0)=1$. One can see that in $\mathbf{e}_x$ polarization the frequency splitting $\Omega(x)$ consists of two positive parts. One is determined by the magnetic field, and the other one is determined by the polariton effect and depends on the sign of x. The phase angle $\Theta(x)$ consists of three parts including the initial difference of phases φ and two propagation parts, which depend on the magnetic field, on the polariton effect, and on the thickness of the crystal d. This means that for the same value of x, the phase angle Θ and the resultant quasiresonant or periodic behavior of the light intensity is different in the crystals of different thicknesses depending on the magnetic field strength. Now we will use the model of the quadrupole polariton in Cu_2O crystal discussed in Ref. 12. It is characterized by the span of the polariton branches and by the splitting between the UPB and LPB. In the intersection point k_0 of the bare $1S$, Γ_5^+ exciton level and photon branch the value of this splitting was evaluated approximately as 100 μeV. The homogeneous damping $\Gamma=2\gamma$ in this model was taken to be 0.9 μeV and the total g factor $|g_c+g_v|$ was taken as 1.78. We will see how these parameters can be changed to obtain better agreement with the experiment. The difference of phases $\varphi=\varphi_2-\varphi_1$ of two coherent polariton waves is $-\pi$ in the case of condensed mixed states of excitons and photons.[27,36] It is the same in our case, because the properties of coherent macroscopic waves and classical waves coincide. Gathering the expressions (44), (45), (61), and (62) one obtains the full set of necessary formulas describing the propagation Hanle effect. For the sake of simplicity we will put $I_1=I_2=I$ and $p_1=p_2=p$ and will calculate the expression

$$\mathcal{A}\equiv\frac{J(p(x),\Theta(x,y),b(x,y))}{2Ip(x)}$$
$$=J_c(p(x),0)+\cos\Theta(x,y)J_c(p(x),b(x,y))$$
$$+\sin\Theta(x,y)J_s(p(x),b(x,y)). \quad (63)$$

The expressions $\Theta(x,y)$, $b(x,y)$, and $p(x)$ are

$$\Theta(x,y)=\Theta(x,y;\zeta,\sigma)=\zeta\left[0.7y+\frac{13.56x\sigma}{\sqrt{1-x^2}}\sqrt{\frac{\sigma+0.1y}{\sigma+0.2y}}\right]+\pi,$$

$$b(x,y)=b(x,y;q,\sigma)=q\left[\frac{0.028y}{(1+x)}+\frac{0.271\sigma}{\sqrt{1-x^2}}\sqrt{\frac{\sigma+0.1y}{\sigma+0.2y}}\right],$$

$$p(x)=p(x:q,r)=\frac{2.44\times10^{-3}qr}{1+x}, \quad (64)$$

where y and the parameters x, q, r, and σ and ζ are introduced as follows:

$$H_0=0.1yT=10^3y \text{ G}, \quad d=0.5\zeta \text{ cm},$$

$$v_g=\frac{c}{2}(1+x), \quad c=\frac{c_0}{\sqrt{\epsilon_\infty}}, \quad \epsilon_\infty=6.5,$$

$$v_g=0.59\times10^{10}(1+x) \text{ (cm/sec)},$$

$$\Delta\omega=v_g\,\Delta k=5.9\times10^{11}\frac{(1+x)}{q}(\text{sec}^{-1}),$$

$$\Delta k=\frac{10^2}{q} \text{ (cm}^{-1}),$$

$$2\hbar\gamma=0.9r(\mu \text{ eV}), \quad 2\gamma=1.44\times10^9 r\,(\text{sec}^{-1}),$$

$$\sqrt{F}=\sqrt{F_0\,\eta(H_0)}, \quad \hbar\sqrt{F_0}=100\sigma \text{ } (\mu \text{ eV}),$$

$$\sqrt{F_0}=1.6\sigma\times10^{11} \text{ (sec}^{-1}),$$

$$\eta(H_0)=\frac{\sigma+0.1y}{\sigma+0.2y}, \quad |g_c+g_v|=1.78,$$

$$\mu_B=0.93\times10^{-20} \text{ (cgs)},$$

$$\tau_{pr}=\frac{0.85\times10^{-10}\zeta}{1+x} \text{ (sec)}, \quad \tau_{coh}=\frac{7}{r}10^{-10} \text{ (sec)},$$

$$2\omega_L=1.655y\times10^{10} \text{ (sec}^{-1}), \quad \frac{2\omega_L}{\Delta\omega}=0.028\frac{q\cdot y}{1+x},$$

$$\frac{\sqrt{F_0}}{\Delta\omega}=0.27\frac{q\sigma}{1+x}. \quad (65)$$

Snoke, Wolfe, and Mysyrowicz[37] observed the anomalous ballistic $1sY$ exciton propagation and the existence of stable envelope wave packets below some critical temperature at a given level of excitation as well as above some critical level of excitation at a given temperature in Cu_2O crystal (see also papers by Fortin *et al.*,[38] Mysyrowicz *et al.*,[39] and Fortin and Mysyrowicz[40]). The wave number width Δk of these wave packets was about 10^2 cm^{-1}. In our theoretical evaluation of Δk we take the same order of magnitude. From Eqs. (62), one can see that the trigonometric functions change periodically as a function of the magnetic field strength H_0. This periodicity approximately has the period

$$\Delta H_0=\frac{2\pi\hbar c}{d|g_c+g_v|\mu_B}, \quad (66)$$

which means a periodicity of the trigonometric functions in dependence on the variable y with the period Δy equal to 9, when the thickness of the sample d equals to 0.5 cm and the total g factor equal to 1.78. This can be observed when the magnetic field strength changes in intervals of 1 T. When $d=0.1$ cm, the period Δy equals 45 and the periodicity can

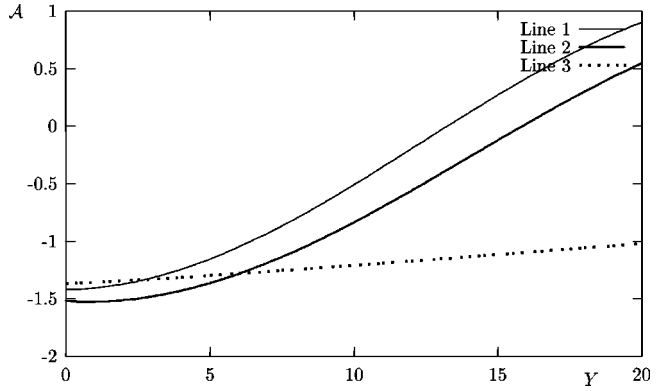

FIG. 3. The light intensity vs the magnetic field strength. Line 1 corresponds to $x=0.1$, $q=1$, $\sigma=1$, $\zeta=0.2$, and $r=1$. Line 2 corresponds to $x=-0.2$, $q=1$, $\sigma=0.2$, $\zeta=0.2$, and $r=10$. Line 3 corresponds to $x=0.1$, $q=1$, $\sigma=1$, $\zeta=0$, and $r=1$.

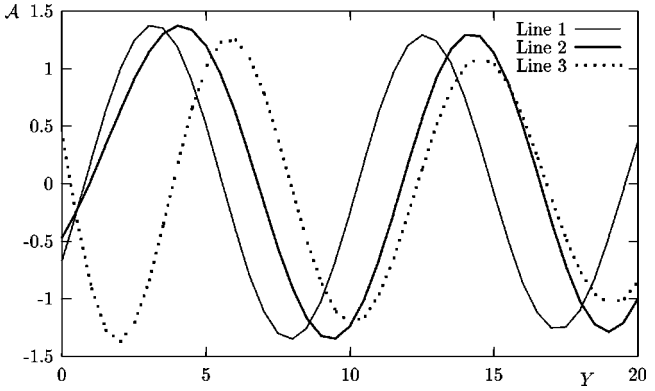

FIG. 5. The light intensity vs the magnetic field strength. Line 1 corresponds to $x=0.1$, $q=1$, $\sigma=1$, $\zeta=1$, and $r=1$. Line 2 corresponds to $x=0.5$, $q=1$, $\sigma=1$, $\zeta=1$, and $r=1$. Line 3 corresponds to $x=-0.5$, $q=1$, $\sigma=1$, $\zeta=1$, and $r=1$.

be observed only in the much greater interval of the magnetic field, about 4.5 T. Let us illustrate this by the numerical example shown in Fig. 3. We start with the case $d=0$, when the propagation effects are completely excluded. The phase angle Θ equals π, which guarantees the increasing character of the quasiresonant dependence on H_0. But the slope of this dependence is small; see Eq. (44) for a definition of the parameter b. When d increases and equals to 0.1 cm, which means $\zeta=0.2$, the character of the dependence remains the same but with increasing slope. This means that the periodicity appears, though the period $\Delta y=45$ is very large. Other parameters x, r, q, and σ have a negligible influence. In Fig. 4 two curves corresponding to $\zeta=0.5$ and $d=0.25$ cm are shown. They demonstrate explicitly the appearance of the periodic dependence with the period $\Delta y=18$, which prevails over the quasiresonant behavior. Now the influence of other parameters is considerable. For example, the increase of the damping constant by one order of magnitude ($r=10$) leads to the decrease of the amplitude of the oscillations, whereas the change of the group velocity parameter x influences on the starting value of the resultant curve at the point $H_0=0$. More evident periodic dependence is demonstrated by three curves in Fig. 5. They correspond to $\zeta=1$, which means $d=0.5$ cm and the period $\Delta y=9$. This periodicity can be observed when the magnetic field strength changes in the interval of 1 T. In this case influence of the parameters x, q, r, and σ is much more important and even can change the slope's sign at the initial part of the curve. If one compares the curves in Figs. 3, 4, and 5 with the experimental results,[19] one can notice that only the quasiresonant dependence in the interval of about 0.5 T was observed though the sample thickness was considerable, $d=0.5$ cm. We believe that for such thicknesses the periodic dependence could be observed. A possible explanation of this discrepancy is the necessity to take into account the time needed for the quadrupole polariton formation. It is determined by $(\sqrt{F})^{-1}$ and the order of magnitude is 10^{-11} sec. During this time light propagates about 0.1 cm. Presumably, the quadrupole polariton wave packets appear after the band-to-band transition and electron-hole pair creation with such a time delay and begin to propagate, starting on the inner surface inside the crystal, but not on the external illuminated side, as one can expect. By these reasons the effective propagation way for them can be less than the crystal thickness.

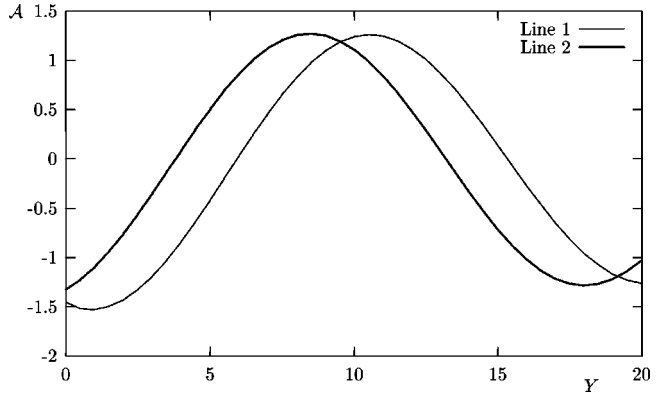

FIG. 4. The light intensity vs the magnetic field strength. Line 1 corresponds to $x=-0.2$, $q=1$, $\sigma=0.2$, $\zeta=0.5$, and $r=10$. Line 2 corresponds to $x=0.1$, $q=1$, $\sigma=1$, $\zeta=0.5$, and $r=10$.

The developed theory is applicable if the main condition $v_g>2\gamma d$ holds. This means the existence of a group velocity cutoff from below, so that the propagation time is less than the coherence time $\tau_{pr}<\tau_{coh}$. In all the cases considered in Figs. 3, 4, and 5 these conditions fulfilled. Another condition is the restriction of comparably small magnetic fields determined by the inequality $2\omega_L\leqslant\sqrt{F_0(k_0)}$. This means that the polariton effect even in the case of quadrupole transitions prevails Zeeman splitting of the ortho-exciton level. All necessary parameters describing this system are given by Eq. (66). The magnetic field strengths up to 1 T obey this requirement. In the experiment[19] the magnetic field was inside the above-mentioned interval, but the calculations were made for the values of 2 T, where, strictly speaking, the approximation (54) is not applicable, but can be treated as an extrapolation. Another problem is the possibility to take into account simultaneous propagation of many pairs of wave packets with different group velocities, obeying the main criterion discussed above. These aspects will be studied elsewhere.

ACKNOWLEDGMENTS

The results of the present studies were reported at the joint seminar of the Institute of Physics and of the Institute of Semiconductor Physics of the National Academy of Sciences of Ukraine in Kiev. One of the authors (S.A.M.) is grateful to Professor I. V. Blonskii and to all participants at the Kiev seminar for valuable discussions and remarks, as well as to his colleagues Professor P. I. Khadzhi, Dr. Sc. I. V. Beloussov, Dr. M. I. Shmiglyuk, Dr. S. S. Russu, and L. V. Arapan for the fruitful discussions and assistance during the work. The U.S.-Moldova Collaboration and the financial support (Contract No. 7380) and the grant of the Highest Council for Science and Technological Development of Republic of Moldova are acknowledged. Another author (M.A.L.) gratefully acknowledges support of this work given by the Swedish Natural Science Research Council (NFR), by the Swedish Research Council for Engineering Sciences (TFR), and by the Swedish Royal Academy of Sciences.

[1] W. Hanle, Zs. fr Fysik **30**, 93 (1924).
[2] L. N. Novikov, G. V. Scrotskii, and G. I. Solomakho, Sov. Phys. Usp. **113**, 597 (1974).
[3] L. N. Novikov, V. G. Pokazan'ev, and G. V. Scrotskii, Sov. Phys. Usp. **101**, 273 (1970).
[4] G. E. Pikus and E. L. Ivchenko, in *Excitons*, edited by E. I. Rashba and M. D. Sturge (Nauka, Moscow, 1985), Chap. 6.
[5] G. Lampel, Phys. Rev. Lett. **20**, 491 (1968).
[6] R. R. Parsons, Phys. Rev. Lett. **23**, 1122 (1969).
[7] B. P. Zakharchenya, V. G. Fleisher, R. I. Djioev, and Iu. P. Veshchunov, Pis'ma Zh. Eksp. Teor. Fiz. **13**, 195 (1971).
[8] E. F. Gross, A. I. Ekimov, B. S. Razbirin, and V. I. Safarov, Pis'ma Zh. Eksp. Teor. Fiz. **14**, 108 (1971).
[9] M. Nawrocki, R. Planel, and C. Benoit a la Guillaume, Phys. Rev. Lett. **36**, 1343 (1976).
[10] R. Planel, M. Nawrocki, and C. Benoit a la Guillaume, Nuovo Cimento Soc. Ital. Fis., B **39**, 519 (1977).
[11] D. Fröhlich, A. Kulik, B. Uebbing, A. Mysyrowicz, V. Langer, H. Stolz, and W. von der Osten, Phys. Rev. Lett. **67**, 2343 (1991).
[12] D. Frohlich, A. Kulik, B. Uebbing, V. Langer, H. Stolz, and W. von der Osten, Phys. Status Solidi B **173**, 31 (1992).
[13] V. Langer, H. Stolz, W. von der Osten, D. Frohlich, A. Kulik, and B. Uebbing, Europhys. Lett. **18**, 723 (1992).
[14] V. Langer, H. Stolz, and W. von der Osten, Phys. Rev. B **51**, 2103 (1995).
[15] H. Stolz, Phys. Status Solidi B **173**, 99 (1992).
[16] A. Z. Genack, H. Z. Cummins, M. A. Washington, and A. Compaan, Phys. Rev. B **12**, 2478 (1975).
[17] J. L. Birman, Phys. Rev. B **9**, 4518 (1974).
[18] W. von der Osten, V. Langer, and H. Stolz, in *Coherent Optical Interactions in Semiconductors*, Vol. 330 of NATO Advanced Study Institute, Series B: Physics, edited by R. Phillips (Plenum Press, New York, 1994).
[19] S. Kono and N. Nagasawa, Solid State Commun. **110**, 159 (1999).
[20] S. A. Moskalenko, A. I. Bobrysheva, and E. S. Kiselyova, Phys. Status Solidi B **213**, 377 (1999).
[21] L. P. Gor'kov and I. E. Dzyaloshinskii, Zh. Eksp. Teor. Fiz. **53**, 717 (1967) [Sov. Phys. JETP **26**, 449 (1968)].
[22] C. Schefer, *Optika*, Vol. III of *Teoreticheskaya Fizika* (GONTI, Moscow-Leningrad, 1938), Pt. 2, Chap. XII.
[23] Ch. J. Pethick and H. Smith, *Bose-Einstein condensation in Dilute Gases* (Cambridge University Press, New York, 2001).
[24] M. H. Anderson, J. R. Ensher, M. R. Matthews, and C. E. Wieman, Science **269**, 198 (1995).
[25] D. I. Blokhintsev, *The Basis of Quantum Mechanics* (Nauka, Moscow, 1950).
[26] W. C. Tait and R. L. Weiher, Phys. Rev. **166**, 769 (1968).
[27] S. A. Moskalenko and D. W. Snoke, *Bose-Einstein Condensation of Excitons and Biexcitons and Coherent Nonlinear Optics with Excitons* (Cambridge University Press, New York, 2000).
[28] S. A. Moskalenko, *Introduction to the Theory of High Density Excitons* (Shtiintsa, Kishinev, 1983).
[29] S. A. Moskalenko, M. I. Shmiglyuk, and B. I. Chinik, Fiz. Tverd. Tela (Leningrad) **10**, 351 (1968).
[30] A. L. Ivanov and L. V. Keldysh, Zh. Eksp. Teor. Fiz. **84**, 404 (1983).
[31] M. S. Brodin, D. B. Goer, and M. G. Matsko, Pis'ma Zh. Eksp. Teor. Fiz. **20**, 300 (1974).
[32] V. R. Misko, S. A. Moskalenko, A. H. Rotaru, and Yu. M. Shvera, Phys. Status Solidi B **159**, 477 (1990); Zh. Eksp. Teor. Fiz. **99**, 1215 (1991).
[33] L. V. Keldysh and S. G. Tikhodeev, Zh. Eksp. Teor. Fiz. **90**, 1852 (1986): **91**, 78 (1986).
[34] P. I. Khadzhi, *The Probability Function (Integrals, series and some generalizations)* (The Academy of Sciences of MSSR, Kishinev, 1971).
[35] I. S. Gradshtein and I. M. Ryzhik, *Tables of Integrals, Sums, Series and Products* (Nauka, Moscow, 1959).
[36] S. A. Moskalenko, M. F. Miglei, M. I. Shmiglyuk, P. I. Khadzhi, and A. V. Lelyakov, Zh. Éksp. Teor. Fiz. **64**, 1786 (1973) [Sov. Phys. JETP **37**, 902 (1973)].
[37] D. Snoke, J. P. Wolfe, and A. Mysyrowicz, in *Bose-Einstein Condensation*, edited by A. Griffin, D. Snoke, and S. Stringari (Cambridge University Press, Cambridge, England, 1994).
[38] E. Fortin, S. Fafard, and A. Mysyrowicz, Phys. Rev. Lett. **70**, 3951 (1993).
[39] A. Mysyrowicz, E. Fortin, and E. Benson, Phys. Rev. Lett. **77**, 896 (1996).
[40] E. Fortin and A. Mysyrowicz, J. Lumin. **87-89**, 12 (2000).